Disc. 106-S15/From the March-April 2009 *ACI Structural Journal*, p. 142

Adaptable Strut-and-Tie Model for Design and Verification of Four-Pile Caps. Paper by Rafael Souza, Daniel Kuchma, JungWoong Park, and Túlio Bittencourt

Discussion by Andor Windisch

ACI member, PhD, Karlsfeld, Germany

Referring to the problems at the application of the sectional approach, the authors propose strut-and-tie models to predict the behavior of four-pile caps. A reasonable doubt is that the sectional approach "exaggerates the importance of the effective depth for calculation shear strength." It is true that in D-regions, the inner lever arm is less than in B-regions. Nearly all specimens of the numerous test programs, even if their failures were proclaimed as by shear, were preceded by the yielding of longitudinal reinforcement, that is, were caused by poor bending capacity. Nevertheless, during the entire paper, the authors make use of *d*, the "effective depth" of pile caps, which is really not effective in a D-region. Accordingly, the shear span-depth ratios, the mechanical reinforcement ratios, and the normalized shear stresses, as defined and used in Fig. 1 to 3, yield misleading interdependencies.

STRUT-AND-TIE MODEL TO PREDICT BEHAVIOR OF FOUR-PILE CAPS

The strut-and-tie model (STM) shown in Fig. 4 raises the following questions/concerns:

- As mentioned previously, the real effective depth differs from the geometrical defined depth *d*. (In their concluding remarks, the authors refer correctly to the unknown position of the nodal zone underneath the column, but give no guidance.)
- For what reasons were no bottle-shaped compression struts chosen?
- The ties of the proposed STM do not fulfil the requirement of the minimum internal work: ties along the diagonals A-D and B-C would yield less energy. Moreover, especially if the pile cap has a cuboid geometry, the first cracks develop in the center of the cap, just under the column, hence the reinforcing bars positioned along the diagonals would most efficiently control the behavior of the cap.
- The same diagonal reinforcement layout must be proposed when the pile-cap is turned upside down: the four piles load the column at the corners of a bracket-like plate. This interpretation makes the punching failure found by Blevót and Frémy[14] understandable.

Due to the aforementioned problem with the "effective depth," both fundamental equations (Eq. (2) and (4)) are questionable. The parameter ϕ_y in Eq. (5) may refer to, among others, the ratio of real effective depth to depth *d*.

Being in a D-region, the expression for the axial load to produce the first cracks given by Eq. (11) is questionable, too.

CONCLUDING REMARKS

For the design of pile caps, both the sectional design method and the strut-and-tie-method could be applied and both have the same Achilles' heel (as correctly remarked by the authors): to find the real effective depth. This immediately solves the problem with the "complex and nonlinear strain distribution throughout the pile cap." Pile caps, similar to short brackets or deep beams, never fail in shear. The STM describes it with the direct compression struts' flow. The sectional design on the other side does not need to take care of the shear problem. As the authors properly state, the so-called shear failures occurred after yielding of the longitudinal reinforcement. This means weak flexural reinforcement. At STM, the inclination of the inclined compression strut defines the amount of the necessary flexural reinforcement. This is hidden behind the recommendation given by the authors: "to prevent this sort of failure, a compressive stress under $1.0f_c$ and a relation shear span-depth ratio under 1.0 normally can lead to ductile failures." The conclusion of Nori and Tharval[28] must be agreed upon: any reduction of the amount of longitudinal reinforcement results in a brittle failure of the pile cap.

The authors are correct in the following:

- It is difficult to generalize the fact that strut-and-tie is more economical.
- The tensile contribution of the concrete is underestimated by the application of either the sectional design methods or the strut-and-tie design provisions for very stocky pile caps.
- Improved models are needed that can account for compatibility and tensile contributions of concrete materials.

Comparative tests are needed with diagonally reinforced pile caps.

AUTHORS' CLOSURE

The authors would like to thank the discusser for his interest in the paper, for his positive comments, and for providing the authors the opportunity to clarify some issues of the paper.

Initially, the authors agree with the discusser that using the effective depth for calculating shear strength of pile caps can lead to unrealistic results, mainly when using a sectional approach. This fact was inclusively confirmed by experimental results obtained by one of the author's references.

On the other hand, the discusser has mentioned that the authors have used the same effective depth to develop a strut-and-tie model for four-pile caps and it raises some doubts regarding the validity of the model. Also, the discusser points out that the inner level arm in a D-region will be less than the one realized in a B-region.

In the authors' opinion, it is not possible to generalize the fact that the effective depth in a D-region will be less than in a B-region, as these regions have totally different behaviors. In the case of pile caps, for example, one may find the same internal level arm between horizontal compressive struts

(top of the pile cap) and tension steel ties (bottom of the pile cap), using the sectional approach (B-region) or a strut-and-tie model (D-region).

Some design codes permit the use of the sectional approach for design pile-caps. In fact, there is no major problem when designing the reinforcement using this method as it normally leads to differences of approximately 20% regarding a strut-and-tie model. The sectional approach, however, is not adequate for previewing the shear behavior of stocky pile caps (span-depth ratio of less than 2, in general) once it is deeply related to the effective depth. If the effective depth is increased, the expected shear loads will be higher; it is not true for a D-region designed using the sectional approach.

For a D-region, when the depth of the pile cap is increased, the diagonal struts will tend to pass from a situation of prismatic struts to bottled-shaped struts, which is a form of strength penalty, as compressive bottled-shaped struts are subjected to splitting. In fact, the authors have used the effective depth in their proposal; however, the increase in this value is subject to a penalty through Eq. (7) through (9).

Regarding the position of the nodal zone underneath the column, the authors believe it is really a value of high uncertainty. This position, however, may be estimated based on the recommendation of Paulay and Priestley.[31] In their opinion, the effective depth of the horizontal strut underneath the column may be taken as $h/4$, where h is the total height of the pile cap.

The authors are working on new and more complete models[13] (refer to Fig. 5) where the position of the nodal zone underneath the column, the diagonal bottled-shape struts, compatibility equations, and compression softening effects are considered. The discusser may find further clarification in the referred paper.

Regarding the position of the ties, the authors agree with the discusser that the proposed layout in the strut-and-tie model will require more reinforcement than a situation of diagonal positioning of the reinforcement. However, one should remember that the proposed model attempts to predict the behavior of some data collected from experimental research. In the majority of these tests, and even in practical and real situations, the proposed layout is preferred. Also, a minimum grid of reinforcement is usually distributed in the bottom of pile caps to prevent premature cracks that may develop in the center of the cap.

The authors agree with the discusser that diagonally reinforced pile caps should be tested. The number of tests

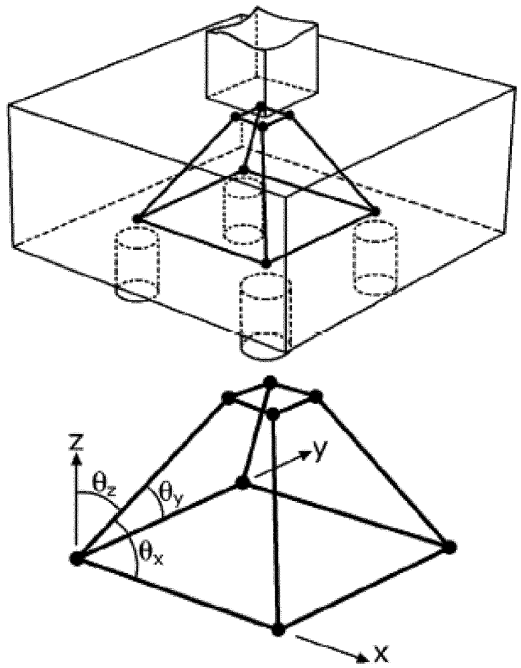

Fig. 5—Strut-and-tie model for four-pile caps proposed by Park et al.[13]

available to effectively describe the behavior of pile caps is very small. Besides that, the available results do not represent the reality of what the pile caps are usually subjected to in construction. The majority of the collected data refers to four-pile caps supporting square columns subjected to axial force. In fact, in most situations, pile caps tend to support rectangular columns subject to axial load and biaxial flexure. New models taking into account this reality need to be developed to adequately address the economy and safety aspects of pile caps.

Finally, the authors recommend the use of the strut-and-tie model for pile caps with span-depth ratios of less than 2. The sectional approach may yield better results for pile caps with large span-depth ratios, that is, span-depth ratios greater than 2.

REFERENCES

31. Paulay, T., and Priestley, M. J. N., *Seismic Design of Reinforced Concrete and Masonry Buildings*, second edition, John Wiley and Sons, New York, 1992, 768 pp.

Disc. 106-S17/From the March-April 2009 *ACI Structural Journal*, p. 160

Two-Way Shear Strength of Slab-Column Connections: Reexamination of ACI 318 Provisions. Paper by Widianto, Oguzhan Bayrak, and James O. Jirsa

Discussion by John Gardner

Professor Emeritus, University of Ottawa, Ottawa, ON, Canada

The authors have given an excellent description of the historical development of the punching shear provisions of ACI 318. However, the section on previous research on two-way shear resistance of slabs refers to only 16 of the references listed. Additional references worth review include Kinnunen and Nylander,[65] Shehata and Regan,[66] Shehata,[67] Gardner,[68] Alexander,[69] Silfwerbrand and Hasssanzadeh,[70] and Sundquist.[71] The addition of the authors' tests results to the literature is welcomed; however, the punching shear capacities for the two slabs reported, G0.5 and G1.0, are lower than the discusser would expect.

Comparison of code provisions with experimental results is not straightforward because the code provisions were designed to be conservative, use specified or characteristic concrete strength and not the mean strength reported for the experimental studies, and sometimes include hidden factors

in the equation coefficients. Code prediction equations should be capable of direct verification against experimental results. The larger shear perimeters of BS8110-97,[64] DIN 1045-1[51] and Eurocode 2[62] are advantageous for concentric punching shear but create difficulties in interpretation for edge and corner slab-column connections.

Prior to 1984, the punching shear provisions of CSA A23.3 were similar to those of ACI 318. CSA A23.3-84M[71] replaced the ACI behavior factor φ with material partial safety factors $\varphi_c = 0.6$ and $\varphi_s = 0.85$, and changed the load factors to $1.25D + 1.5L$. To maintain the same level of safety as the previous code, the coefficients in the punching shear expressions were increased by 21% (CSA A23.3.84M, Clause B3(b)). CSA A23.3-04[52] increased the concrete material factor φ_c to 0.65 and reduced the equation coefficients by 5%. Changing the equation coefficients is poor practice, as setting $\varphi_c = \varphi_s = 1$ in the strength capacity equation should give the 95% lower bound of a population of test/predicted results.

BS8110-97,[64] CEB MC90,[63] DIN 1045-1,[51] and Eurocode 2[62] use material factors $\phi > 1$ in the denominator, whereas ACI and CSA use $\phi < 1$ in the numerator. DIN 1045-1 does not state explicitly that the material understrength factor $\gamma_c = 1.5$ is included in the equation coefficients, but Hegger et al.[73] wrote the equation coefficient as $0.21/\gamma_c$. The punching shear capacities, calculated using mean concrete strength, the revised coefficient, and $\phi = \gamma_c = \gamma_m = 1$, are given in Table 4. Using specified, or characteristic, concrete strength would reduce the calculated capacities.

The conclusion that DIN 1045-01[51] is conservative is incorrect—none of the code expressions are conservative. However, as stated previously, the punching shear capacities for the two slabs reported, G0.5 and G1.0, are lower than the discusser would expect.

The conclusions based on experimental research at the University of Texas at Austin are too broad considering that only two slabs were tested. However, Fig. 3 of Reference 68 shows that the ACI 318 punching shear equations are not conservative for reinforcing ratios less than 0.7%.

REFERENCES

64. Kinnunen, S., and Nylander, H., "Punching of Concrete Slabs without Shear Reinforcement," *Transactions of the Royal Institute of Technology (KTH)*, Stockholm, No. 158, 1960, 110 pp.

65. Shehata, I. A. E. M., and Regan, P. E., "Punching in Reinforced Concrete Slabs," *Journal of Structural Engineering*, ASCE, V. 115, No. 7, 1989, pp. 1726-1740.

66. Shehata, I. A. E. M., "Simplified Method for Estimating the Punching Resistance of Reinforced Concrete Slabs," *Materials and Structures*, V. 23, No. 137, 1990, pp. 364-371.

67. Gardner, N. J., "Punching Shear Provisions for Reinforced and Prestressed Concrete Flat Slabs," *Canadian Journal of Civil Engineering*, V. 23, No. 2, Apr. 1996, pp. 502-510.

68. Alexander, S. D. B., "Strip Design for Punching Shear," *The Design of Two-Way Slabs*, SP-183, T. C. Schaeffer, ed., American Concrete Institute, Farmington Hills, MI, 1999, pp. 161-179.

69. Silfwerbrand, J., and Hasssanzadeh, G., "International Workshop on Punching Shear Capacity of RC Slabs—Proceedings," TRITA-BKN, *Bulletin* 57, KTH, Stockholm, 2000, 517 pp.

70. Sundquist, H., "Punching Research at the Royal Institute of Technology (KTH) in Stockholm," *Punching Shear in Reinforced Concrete Slabs*, SP-232, M. A. Polak, ed., American Concrete Institute, Farmington Hills, MI, 2005, pp. 229-257.

71. CSA A23.3-M84, "Design of Concrete Structures," Canadian Standards Association, 1984, pp. 232-234.

72. Hegger, J.; Sherif, A.; and Beutel, R., "Punching of Reinforced Concrete Flat Slabs—ACI and German Guidelines," *Punching Shear in Reinforced Concrete Slabs*, SP-232, M. A. Polak, ed., American Concrete Institute, Farmington Hills, MI, pp. 209-228.

Table 4—Calculated punching shear capacities for Widianto slabs (calculated using mean concrete strength)

Code	Expt., kips (kN)	ACI 318-05,* kips (kN)	BS 8110-97,[64] kips (kN)	EC2,[62] kips (kN)	DIN 1045-1,[51] kips (kN)	Gardner,[67†] kips (kN)
Slab G0.5	69.9 (310.9)	112.6 (501)	86.1 (383)	93.5 (416)	95.5 (425)	75.3 (335)
Slab G1.0	90.2 (401.2)	106.5 (474)	104.6 (454)	113.5 (505)	116.0 (516)	91.2 (406)

*Square perimeter used.
†Steel yield strength taken as 70 ksi (480 MPa).

AUTHORS' CLOSURE

The authors would like to thank the discusser for his interest and comments. As implied by the title of the paper, the focus was on ACI 318 provisions. This focus was stated in the Research significance section, detailed in the main body of the paper and reiterated in the Conclusions section. The objective of the paper was neither to examine nor to report on all design codes, all analytical formulas, and/or all test results ever published.

The low shear strength values recorded in the authors' tests should not be too surprising, considering the fact that there are many test results reported in the literature[14,30,31,33,37,39] that are approximately the same as those for Specimens G0.5 and G1.0. Even though the focus of the paper was on ACI 318 provisions, the authors presented different code provisions only to illustrate "the diverging approaches used for the code equations" and the fact that mechanics of punching shear failure have not been well understood. By these illustrations, the authors wanted to convey the message that reexamination of the ACI 318 provision for two-way shear strength (which has not changed since 1963) is warranted.

The discusser indicated that "DIN 1045-1 does not state explicitly that the material understrength factor $\gamma_c = 1.5$ is included in the equation coefficients, but Hegger et al.[73] wrote the equation coefficient as $0.21/\gamma_c$." The authors have presented the equations that were taken directly from DIN 1045-1[51] in Table 2. Similar to DIN 1045-1,[51] the authors also used the equations as they appear in the BS 8110-97[64] and Eurocode 2.[62] The comparative evaluation of various code provisions and experimental results is not straightforward and was highlighted in the section titled "Building code provisions: comparison":

> The shear strength varies from about 480 kN using German Code DIN 1045-1[42] to over 1100 kN using Canadian Standards CSA A23.3-04[43] for slabs with a 0.5% flexural reinforcement ratio. Some of these differences may be reduced if load or understrength factors are included. However, the variations indicate the diverging approaches used for the code equations.

The statement made regarding DIN 1045-1[51] seems to have been misinterpreted. The reported conclusions are only related to the two specimens tested at the University of Texas at Austin. It is explicitly stated in the Conclusions section of the original paper that: "Unlike other building codes, DIN 1045-1[51] provided a 20% conservative estimate of the capacity for the connection tested" for Specimen G0.5 and "The capacity of Specimen G1.0 (which represents a

slab-column connection in typical flat-plate structures built to meet current standards) was also overestimated (between 9 and 36%) by all but DIN 1045-1.[51] It should also be noted that the Conclusions contained the following statement: "Based on the results of experimental research conducted at the University of Texas at Austin, the following observations can be made." Certainly, strength estimates may change if load or understrength factors are included.

Finally, it is stated in the "Recommendations" section of the original paper that, "The overwhelming evidence gathered from the literature[14,37,39-44] and obtained in the experimental program[1] illustrates that the use of ACI 318 provisions for lightly-reinforced slab-column connections is questionable." The conclusions presented were based on experimental research at the University of Texas at Austin and test results reported in the literature.

Disc. 106-S18/From the March-April 2009 *ACI Structural Journal*, p. 171

Behavior of High-Performance Steel as Shear Reinforcement for Concrete Beams. Paper by Matthew S. Sumpter, Sami H. Rizkalla, and Paul Zia

Discussion by Andor Windisch

ACI member, PhD, Karlsfeld, Germany

In the introduction, the authors correctly point out that using high-performance steel in comparison with conventional steel could potentially relieve congestion in future structures. Nevertheless, it is odd that, for the nine reinforced beams, the same cross-sectional areas for longitudinal and shear reinforcement were applied without depending on the strength of the steel. This means that even the flexural beams' test results cannot be accurately compared to each other, as the tensile forces and the concrete compression zones are completely different. Choosing the same cross-sectional area for the longitudinal MMFX bars, the authors want to keep the effect of dowel action constant. This is a questionable decision for two reasons:

1. The purpose of using high-strength steel is to reduce bar diameters.

2. The dowel action is not considered at all, neither in the codes nor in the analytical modeling.

Similar problems arise with regard to the transverse reinforcement: the same spacing of the identical diameter reinforcing bar having very different yield strengths results in substantially different test beams. Hence, any behavior characteristics of, for example, Beams C-C-6, C-M-6, and M-M-6 test cannot be compared with each other.

Another curiosity is the application of the high-strength steel in the compression zone: the strain compatibility between concrete and high-strength steel and, hence, the applicability of MMFX as compressive reinforcement, is more than questionable.

TEST RESULTS

It is a pity that for each type of behavior, the test results of only one set are shown. Thus, no detailed perception of the varied characteristics is possible for the reader.

Due to the disputable substitution of ordinary steel through high-strength steel, as mentioned previously, the sets of test beams and the percents of increase, as shown in Table 1, are not meaningful. Nevertheless, the values in the column "Percent total increase," reveal no tendency and could yield the conclusion that the substitution as proposed by the authors is not sensible.

Another possibility for formation of groups and evaluation can be made based on the ratios of yield strengths and the spacings of transverse steel. Taking into account the two yield strengths of 97 and 120 ksi (669 and 827 MPa) assessed for the MMFX steel and comparing it to the yield strength of the Grade 60 steel (62 ksi [427 MPa]), two strength ratios can be determined

$$\frac{97}{62} = \frac{690}{427} = 1.61 \quad \frac{120}{62} = \frac{827}{427} \approx 2$$

Considering the spacings of the transverse steel, the ratios 6/4 ~ 1.5 (hence X-C-4 ≈ X-M-6) and 6 / 3 = 2 (hence X-C-3 ≈ X-M-6) can be found. Accordingly, the following sets of beams for comparison can be compiled:

- Ratio of shear reinforcement ~ 2 – Set A: C-C-3, C-M-6, and M6; and
- Ratio of shear reinforcement ~ 1.5 – Set B: C-C-4, C-M-6, and M-M-6.

Moreover, keeping the longitudinal reinforcement constant for Grade 60 and MMFX, the influence of the increasing transverse reinforcement can be perceived:

- Flexural reinforcement constant, increasing – Set C: C-C-6, C-C-4, and C-C-3; and
- Flexural reinforcement constant, transverse reinforcement increasing – Set D: M-M-6, M-M-4, and M-M-3.

Table 4 displays the test results according to the new sets.

The following conclusions can be made:

- The method of normalization of the measured shear strength, that is, with respect to the square root of the concrete compressive strength, is questionable; the values in Column 5 do not show the anticipated increasing character for the different sets.
- Set A: the substitution of the shear reinforcement considering 2 as the ratio of the yield strengths results in similar load-bearing capacities.
- Set B: a substitution considering 1.5 as the ratio of the yield strengths underestimates the contribution of MMFX steel.
- Sets C and D: doubling the rate of shear reinforcement let the ultimate shear load increase by 7 to 11% only.
- For each of these conclusions, it should be kept in mind that the load-bearing capacities of all of the test beams were governed by the concrete compressive strength. Furthermore, besides the higher yield strength, MMFX has much better bond characteristics than ordinary steel.

Shear load-deflection behavior

Figure 6 reveals the impact of longitudinal reinforcement on the ultimate shear load. This effect should be incorporated into the new code provisions.

Shear load-transverse strain behavior

The conclusions related to Fig. 7 are either not new or misleading:

- Certainly both the initiation of the first shear crack as well as of the first flexural crack do not depend on the strength of the reinforcement. In the formula for stiffness, only the cross sectional area and the Young's modulus occur.
- The initiation of the first shear crack using the vertical PI gauge can be perceived only if the crack runs through the gauge length.
- Figure 7 gives the impression that the stirrups made of both the Grade 60 ordinary steel as well as, for example, Grade 120 MMFX steel, would yield, which cannot be the case, especially for the MMFX steel.

The discusser poses a question regarding Fig. 9: Is there any difference in the failure patterns of Beams C-C-4 and C-C-3? In the discusser's opinion, there is not. In all cases, the concrete compression zone fails in compression shear. The upper part of the so-called "diagonal crack at failure," shown in Fig. 9(a) is a sliding surface along the compression zone.

Crack width behavior

The use of average crack width as a criterion is misleading. All codes control an upper fractile value of crack width. Moreover, Shehata's[6] equation does not consider the different bond characteristics of the two types of reinforcement. A direct replacement of conventional steel with ASTM A1035 steel, as done in this test series, makes no sense and, hence, any conclusion here is misleading, too.

The authors should explain why the M-M beams had smaller shear crack widths than the C-M beams.

Mode of failure

The authors wrote: "for both C-M and M-M beams, failure occurred once the compression strain in the diagonal direction reached its ultimate value and led to crushing of the concrete at the nodal zone." The discusser agrees and poses the question: Which level of the compression strain was detected as the ultimate value? Was it the same for all beams?

Effect of steel type

The authors did not find any HP steel-specific characteristics.

ANALYTICAL MODELING

The discusser strongly disagrees that the measured-predicted shear-load ratios found using the program Response 2000 are more accurate than the design code predictions. In five of the nine cases, Response 2000 yielded very unsafe predictions. Considering the six test beams consisting of HP steel, five results were unsafe.

In general, the practice of revealing analytical models yielding average values of approximately 1.00, but with considerable standard deviation that results in lower fractile values strongly below 1.00, as "more accurate" cannot continue.

CONCLUSIONS

1. Direct replacement of conventional Grade 60 stirrups with ASTM A1035 steel stirrups makes no sense.

2. The authors should explain why the ASTM A1035 longitudinal reinforcement increased shear strength.

3 & 4: Taking into account 48 ksi (331 MPa) service stress level and a yield strength of 80 ksi (552 MPa), the rate of exploitation of the real yield strength of HP steel of 120 ksi (827 MPa) reveals that the application of HP steel is not economical.

5. Whether pairing high-strength concrete with ASTM A1035 steel could provide a better use for HP steel is questionable. Increasing the concrete grade decreases the ultimate strain; that is, the strength of HP steel cannot be exploited in compression.

6. The detailed analysis using MCFT, included in Response 2000, provided partly extremely unsafe predictions of the overall shear strength of concrete members reinforced with HP steel in five of six cases.

AUTHORS' CLOSURE

The authors extend their thanks to the discusser for his insightful and constructive discussion, and to provide the authors an opportunity to further clarify the findings of the experimental study. A response to each item of the discussion is presented as follows:

1. The main objective of the study was to determine how direct replacement (bar for bar) of high-performance steel with conventional Grade 60 steel would affect the shear strength of the concrete beam. This choice was made to demonstrate the implications of such a design practice, which has been used by some designers due to the lack of appropriate design provisions developed by standards organizations. The direct replacement applied to both longitudinal steel and to the transverse steel.

2. The selection to include only one typical test result in the paper was due to space limitations of the journal paper. The reader may review full test results in the master's thesis by Sumpter.[5]

3. The small increase in the shear capacity measured for test group "Set 1" is due to the nature of failure, which is controlled by arch action. For Sets 2 and 3, failure was controlled by concrete crushing at the maximum compression zone. The strength for these sets did not increase by the same ratio of steel area, but was observed to show higher relative increases than Set 1. This was due in part to a high *a/d* ratio, which allowed the steel to be better used as opposed to the formation of arch action.

4. The authors acknowledge and appreciate the discusser's alternative method of analysis for a reader's consideration.

5. The authors' believe that shear strength is more directly related to the square root of the concrete compressive strength rather than solely to the concrete compressive strength. This influenced the decision to normalize the data based on the square root. The reader should refer to the total percent increase given in Table 1 to evaluate the strength increase in comparison to the baseline C-C beam for the same stirrup spacing.

6. The authors agree with the discusser that the longitudinal reinforcement should be considered in code provisions.

7. The intention behind Fig. 7 is to highlight the conservative prediction of ACI 318-05 for high-performance steel. The reported initiation of the first crack was determined both by visual inspection and by the reading of PI gauges, which

were designed to catch the first crack. The measured data shown in Fig. 7 reflect redistribution of forces rather than yielding of MMFX steel.

8. The authors agree that failure occurred once the compression strain in the diagonal direction reached its ultimate value.

9. The smaller measured crack widths for beams reinforced with HP steel is the result of better bond characteristics of ASTM A1035 steel due to their rib configuration. References 7 and 8 provide detailed information regarding this behavior.

10. Unfortunately, the compressive strain was not recorded during testing because it was located close to the applied load.

11. The authors agree that statistical data beyond averages should be considered. Therefore, standard deviation as well as the coefficient of variation was used in Tables 2 and 3 to compare how closely Response 2000 predicted the strength of the beams versus other design codes. The results indicate that design codes over-predict the strength of the beams, while Response 2000 yields results closer to the actual strength because it considers the additional resistance provided by the HP longitudinal steel reinforcement and relies on the MCFT for analysis.

12. Test results indicated that the direct replacement of conventional Grade 60 stirrups with ASTM A1035 stirrups increased the shear load capacity of flexural members, as shown in Table 1.

13. At failure, ASTM A1035 may remain in the elastic region and its resistance increases by increasing the applied load. The increase of the tension forces lead to an increase of the forces in the compression zone, the dowel action, and, thus, the overall shear strength.

14. ASTM A1035 steel reduced crack widths to an acceptable level at a higher service level stress due to the type of rib configuration used for their reinforcing bars, while the conventional reinforcement exceeded the 0.016 in. (0.406 mm) limit. This behavior provides overall enhancement of serviceability.

15. Research conducted by NCHRP Project 12-64 has indicated that the ultimate compressive strain of high-strength concrete up to 18 ksi (124 MPa) is equal to or greater than 0.003. Therefore, the use of high-strength concrete with high-performance steel is expected to provide better use of the materials. Achieving stress levels above 80 ksi (550 MPa) in HP compression steel, however, may be limited because concrete would need to be highly confined to maintain strain compatibility.

Disc. 106-S19/From the March-April 2009 *ACI Structural Journal*, p. 178

Investigation of Dispersion of Compression in Bottle-Shaped Struts. Paper by Dipak Kumar Sahoo, Bhupinder Singh, and Pradeep Bhargava

Discussion by Andor Windisch

ACI member, PhD, Karlsfeld, Germany

The authors investigated the maximum transverse tension developing in bottle-shaped struts. They developed the equations of isostatic lines of compression (ILC) for a panel with an aspect ratio equal to 2 and applied them to investigate panels with aspect ratios equal to 1. In the discusser's opinion, the study should have included panels with other aspect ratios.

The authors considered the place with the maximum slope as the position of the resultant transverse tension, this is supposed to be at $x = a$; however, in Fig. 5, to avoid a sharp edge in the ILC, a horizontal tangent was considered. Consequently, Eq. (9) to (10b) and (16) are questionable. In comparison with other theoretical expressions, the authors refer to the formulas in different codes dealing with the bursting forces in post-tensioned anchorage zones, which might be similar to their formulas, but do not characterize the situation of panels with aspect ratios equal to 1, as shown in Fig. 5 and tested (refer to Fig. 7).

Even if, during the tests, transverse compression stresses under the loading and supporting plates were found, the authors adhered to the transverse strain distribution (that is, transverse tensile stresses also under the plates) shown in Fig. 7(b) and derived Eq. (17) and (18), which are, therefore, questionable.

As can be observed in Fig. 9, the failure loads showed a substantial scatter related to the same concentration ratio, which contradicts the authors' assumption that the mean value of the concentration ratio can be considered at calculation of the m value. Nevertheless, the authors should have chosen the larger $1/m$ values corresponding to the different concentration ratios b/a to obtain safer values.

The test results provide interesting information for the users of the strut-and-tie models (and maybe also for the code makers). In Table 2, the test results are listed and regrouped according to different aspects. First of all, in Column 7, the compressive stresses under the shorter bearing plates are shown (certainly, where the authors refer to 0 length, no stress could be calculated; nevertheless, the development of the failure loads P in Column 6 yield proper view of the influence of the considered parameter). In Column 8, the compressive stresses at failure under the shorter loading/supporting plate related to the concrete strength f'_c are shown.

The following trends and conclusions can be found:

- Keeping the length of one the plates constant and increasing the length of the other plate, the following conclusions are contradictory:
  - Lines 1 to 4: In the case of constant 0 mm length, the other plate lengths increased from 0 to 400 mm (15.75 in.): B-2: 0.70 to B-4: 0.15—the failure load did not change and the relative failure stresses decreased (dramatically).
  - Lines 5 to 7: In the case of constant 100 mm (4 in.) lengths, the other plate length increased from 100 to 400: B-5: 0.98 to B-7: 1.30—the failure loads increased and the relative failure stresses also increased.
  - Lines 8 to 10: One plate had a constant 400 mm (15.75 mm) length, the other increased from 100 to 400: B-7: 1.30 to B-9: 0.51—the failure loads increased, the relative failure stresses decreased (quite substantially).
- Having the same plate lengths at both sides, the relative failure stress decreased when the plate lengths increased.
  - Lines 11 to 15: B-11: 1.79 to B-9: 0.51; B-1 with 0 mm length yielded an even higher value than 1.79, that is, the failure loads increased and the relative compressive stresses decreased.
- The mean value of the plate length was constant.
  - Lines 16 and 17: The mean value of length was 50 mm (2 in.)—the failure loads were quite different, that is, the mean value did not properly represent the real situation.

Table 2—Evaluation of experimental results

	Specimen ID	f_c', MPa	Plate length, mm		Concentration ratio b/a	P, kN	Compressive stress under smaller loading plate, N/mm²	Ratio of compressive stress under smaller loading plate to f_c'
			Loaded face	Supported face				
	1	2	3	4	5	6	7	8
1	B-1	36.5	0	0	0	191.8	—	—
2	B-2	32.8	0	100	0.80	228.7	22.87	0.70
3	B-3	35.3	0	200	0.17	221.5	11.08	0.31
4	B-4	36.5	0	400	0.33	223.2	5.58	0.15
5	B-5	33.2	100	100	0.17	325.2	32.52	0.98
6	B-6	31.5	100	200	0.25	402.1	40.21	1.28
7	B-7	36.9	100	400	0.42	481.0	48.10	1.30
8	B-7	36.9	100	400	0.42	481	48.10	1.30
9	B-8	33.7	200	400	0.50	600	30.00	0.89
10	B-9	37.0	400	400	0.67	747.7	18.69	0.51
11	B-1	36.5	0	0	0	191.8	—	—
12	B-11	32.8	50	50	0.08	293.2	58.64	1.79
13	B-5	33.2	100	100	0.17	325.2	32.52	0.98
14	B-10	33.2	200	200	0.33	429.3	21.47	0.65
15	B-9	37.0	400	400	0.67	747.7	18.69	0.51
16	B-2	32.8	0	100	0.08	228.7	—	—
17	B-11	32.8	50	50	0.08	293.2	58.64	1.79
18	B-3	35.3	0	200	0.17	221.5	—	—
19	B-5	33.2	100	100	0.17	325.2	32.52	0.98
20	B-4	36.5	0	400	0.33	223.2	—	—
21	B-10	33.2	200	200	0.33	429.3	21.47	0.65

Note: 1 mm = 0.0394 in.; 1 kN = 0.2248 kip; 1 N/mm^2 = 145 psi.

- Lines 18 and 19: The mean value of length was 100 mm (4 in.)—the failure load of the specimen with the "mean" plate length was larger than for specimens with the different plates.
- Lines 20 and 21: The mean value of length was 200 mm (7.87 in.)—the failure load of the specimen with the "mean" plate length was larger than for specimen with the different plates.

CONCLUSIONS

The proposed theoretical model is questionable, hence, the derived parameter 1/m cannot be accepted. According to the tests reported in the paper, the effective compressive strength of concrete in the strut (as per Section A.3.1 of ACI 318-05, Appendix A) is, in some cases, conservative, but is, in many cases, on the unsafe side.

AUTHORS' CLOSURE

The authors appreciate the discusser's interest in the paper and his critical review of the analytical and experimental results presented therein. The authors' response to the pertinent issues raised in the discussion is as follows.

The analysis presented in the paper is not restricted to square panels alone as is perceived by the discusser. The development of the equations of the isostatic lines of compression (ILCs) and the derivation of the proposed dispersion model are applicable to bottle-shaped struts of all aspect ratios (Fig. 3 and 5). The reason for choosing a square panel for the experimental validation has been explained in the original paper.

The total transverse tension T' in a bottle-shaped strut is essentially independent of the aspect ratio. In Fig. 5, at the point of intersection, the two ILCs emanating from the loaded and the supported ends will have two different tangents and will have two different components of transverse tension. In Eq. (9), it is the transverse tension component in the incremental strip that is integrated and not the area bounded by the incremental strip (Fig. 3 and 5). In Eq. (10a) and (10b), the transverse tensions contributed by the two ends have been algebraically added. The question of the sharp edge in Fig. 5 would not have arisen if the panel length in Fig. 5 along the x-axis had been taken as, for example, twice the panel width. In Fig. 5, a square panel has been considered to resemble the geometry of the experimental panels. As explained in the paper, a square panel presents a special geometry where the two end regions overlap each other completely, causing the line of action of the resultant transverse tensions of the two end blocks to coincide.

It is difficult to accurately measure or rigorously model the transverse stress profile in a bottle-shaped strut. The authors have assumed a simplified triangular stress distribution[22] along the axis of the strut and the transverse compression at the ends has been ignored to compensate for the additional area of the stress diagram under the convex nonlinear stress profile (Fig. 7).

Scatter in the test results was not altogether unexpected and it is more prominent because the number of specimens is relatively small. It can be readily shown that a higher value of 1/m alone does not indicate a larger magnitude of transverse tension. The transverse tension can be calculated from the following expression obtained by combining the ACI 318-05[19] expression for the nominal strength of a bottle-shaped strut and the dispersion model proposed in the paper in Eq. 10(b).

$$T' = \frac{15P}{32}\left(1 - \frac{b_{av}}{a}\right) = \tag{19}$$

$$\frac{15(0.85\beta_s f_c' \times 2bt)}{32}\left(1 - \frac{b_{av}}{a}\right) = 0.8\beta_s f_c' t b_{av}(1 - b_{av}/a)$$

where β_s is the strut efficiency factor and t is the panel thickness (out-of-plane dimension).

A perusal of Eq. (19) clearly reveals that choosing a larger $1/m$ value (by choosing b_s instead of b_{av}), as suggested by the discusser, will not always increase the magnitude of the transverse tension T' and therefore not necessarily be safe.

With reference to Table 2, the authors would like to respond as follows:

1. It is not clear as to how the compressive stresses under the smaller loading plates were calculated in Column 7 for Specimens B-1, B-2, B-3, and B-4, in which the smaller bearing areas are zero. Keeping the plate length on one side of a panel constant, as the plate length was increased on the other side, the cracking load P was observed to increase. The increase in cracking load can be related to the higher average bearing areas. Because the relative failure stresses based on the smaller bearing areas were not showing any trend in the experimental results, the authors' choice of using the average values of bearing areas is justified.

2. Having the same plate lengths on both sides, the relative failure stresses were observed to decrease when the plate length was increased. This is an expected trend because increasing the bearing length while keeping the panel width constant restricts the lateral dispersion of the compressive stress trajectories, which in turn leads to a reduction in the strut efficiency.[23]

3. With reference to Lines 17 through 21 of Table 2, the authors agree that the cracking loads of the pairs of Specimens B-2 and B-11, B-3 and B-5, and B-4 and B-10 do not match well. The zero bearing length in Specimens B-1 through B-4 was simulated by placing a 16 mm (0.63 in.) diameter round bar, and the small bearing area resulted in premature bearing failure. The results of the four specimens having zero plate lengths, B-1 through B-4, therefore produced maximum scatter in Fig. 9. Nevertheless, all the results except one were on the safe side of the predicted trend (Fig. 9).

With reference to the discusser's conclusions, the authors would like to mention that the theoretical model in the paper was derived from first principles and validated with a limited number of experimental tests. The relative failure stresses reported by the discusser in Column 8 of Table 2 at best indicate a value of $0.85\beta_s$, which for plain concrete bottle-shaped struts as per the ACI Code[19] is 0.51. Except for Lines 1 through 4 in Table 2, where the discusser's calculations seem to be incorrect, the relative failure stress in none of the cases falls below 0.51 (Column 8, Table 2). Therefore, the discusser's analysis of the test results in the paper does not seem to support the discusser's conclusion that the effective compressive strength as per Section A.3.1 of ACI 318-05, Appendix A,[19] is unsafe.

REFERENCES

22. Sahoo, D. K., "An Investigation of the Strength of Bottle-Shaped Struts," PhD thesis, Indian Institute of Technology Roorkee, Roorkee, India, 2009, 324 pp.

23. Sahoo, D. K.; Singh, B.; and Bhargava, P., "An Appraisal of the ACI Strut Efficiency Factors," *Magazine of Concrete Research*, V. 61, No. 6, Aug. 2009, pp. 445-456.

Disc. 106-S20/From the March-April 2009 *ACI Structural Journal*, p. 187

Deformation Capacity of Reinforced Concrete Columns. Paper by Hossein Mostafaei, Frank J. Vecchio, and Toshimi Kabeyasawa

Discussion by Andor Windisch

ACI member, PhD, Karlsfeld, Germany

The authors are to be complimented for their interesting attempt to apply the MCFT, which was conceived for short-term monotonic loading only, to estimate the ultimate deformation of columns that failed after cyclic loading.

DERIVATION OF ANALYTICAL MODEL

Apart from the errors in Eq. (7) and (8) (σ should be replaced with ρ), it should be mentioned that a Mohr's circle may never yield either equilibrium or compatibility relationships: it simply gives the possibility to transform the stress (or deformation) components from one coordinate system to another.

To calculate the angle θ, the strains ε_x, ε_y, and ε_2 are necessary; however, the discusser cannot detect where the three values are derived. The principal compression stress pattern with the angle is given in Fig. 4(a). Does Eq. (12) follow this pattern? Please clarify.

The concrete compression softening factor (Eq. (16)) was derived for monotonic loading. Is it valid for heavily alternating loading paths, too? The shear stress transferred by aggregate interlock across a crack surface (Eq. (17)) was found for the monotonic loading path, too. Does it remain valid for alternating loading? Isn't there any softening?

The validity of the formula for average crack spacing was never proven. What average crack spacing can be found for Specimen No. 12 shown in Fig. 8?

In Eq. (19), the average steel stress in the transverse reinforcement is the yield strength. According to the MCFT, this means that the stress and strain in transverse steel in the crack are far beyond the yielding values. Do w and τ_i remain valid in case of yielding transverse reinforcement?

FLEXURE MECHANISM

It is not clear how Eq. (20), (21a), and (21b) containing the Young's modulus of concrete are compatible with the actual and equivalent concrete stresses shown in Fig. 7 (elastic behavior according to the equations and inelastic behavior according to the figure).

PROCEDURES FOR ESTIMATION OF ULTIMATE DEFORMATION

To simplify, the procedure of estimation interpolation for d_f shall be deleted; after so many assumptions, the difference between h and d is negligible.

NUMERICAL EXAMPLES

It is a pity that the authors did not give more details of their calculations in the form of tables. In comparing the analytical and test results shown in Fig. 11, it can be concluded that most of the specimens were still loaded partly far beyond the ultimate drift ratio predicted by the analytical model, that is, no

failure of the specimens occurred. With MCFT, the load-deformation response of reinforced concrete members could be predicted. It would be interesting to learn which analytical drift ratio versus lateral load paths were determined for the different specimens reported in Fig. 11.

AUTHORS' CLOSURE

The authors are thankful to the discusser for raising important comments and questions regarding the axial-shear-flexure interaction methodology presented in the paper. These remarks have been reviewed and the following explanations are provided for clarification of the methodology, accordingly.

DERIVATION OF ANALYTICAL MODEL

The stress and strain relations, expressed in a Mohr's circle in the MCFT and the ASFI methods, correspond to the average stress and strain condition of the shear element. They are employed for compatibility and equilibrium conditions by assuming unit dimensions for the element, as shown in Fig. 5 and 6 of the paper. In other words, equilibrium and compatibility conditions are derived for the entire element; however, they are converted and expressed in the stress and strain fields.

The correct form of Eq. (7) and (8), respectively, are

$$\sigma_x = f_{cx} + \rho_x f_{sx} \tag{32}$$

$$\sigma_y = f_{cy} + \rho_y f_{sy} \tag{33}$$

The crack angle θ is determined in the stress field by solving Eq. (9) and (10), which is incorporated in Eq. (14) and (15)

$$\tan^2\theta = \frac{f_{c1} - f_{cy}}{f_{c1} - f_{cx}} \tag{34}$$

Figure 4(a) was drawn for the assumption related to Eq. (6). It illustrates the pattern of the principal compression stress, and therefore strain, along the entire column. It shows that the principal compression stress and strain at the points along the curve are very close to the value of the compression stress and strain obtained from a section analysis. Therefore, Eq. (6) could represent the maximum compression strain or assume to provide the principal compression strain of the element between the two flexure sections. Equation (34) provides an average value for the entire pattern shown in this figure when only two flexure sections have been selected: one at the end and one at the inflection point.

The approach presented in this paper can be used only to estimate the point of the ultimate capacity, which is the ultimate deformation and load of the column; however, the equations have been derived from a monotonic loading approach. Therefore, although the method presents suitable agreement for the column specimens in Fig. 11, the attempt was not to assess and include the effect of cycling loading. Therefore, for specimens with heavily cyclic loading, the corresponding effects need to be included in the analysis.

In the ASFI method, the crack spacing in the longitudinal direction of the column, S_x, is the same as the hoop spacing. Crack spacing in the transverse direction, S_y, is the maximum distance between the longitudinal bars. These are the average smeared crack spacings and not the maximum values. For specimen No. 12, S_x = 150 mm (6 in.) and S_y = 60 mm (2.4 in.), which yields to S_{cr} = 72 mm (2.8 in.), derived from the analysis at the maximum load stage. Based on the specimen dimension perpendicular to the crack, this means that approximately four cracks could appear on the columns, as is the case for the column specimen in Fig. 8.

Equation (19) provides a maximum limit for shear stress. As mentioned previously, the method proposed in this paper only estimates the load and deformation of the column at the ultimate stage. For specimens containing transverse reinforcement, the lateral load drops as soon as the transverse bars yield and the analysis ends (defining the ultimate load stage).

FLEXURE MECHANISM

Both the flexural and shear models, as well as the MCFT, use a secant stiffness approach for the analysis. The values for the Young's modulus of concrete in Eq. (20), (21a), and (21b) are the inelastic values. They are determined by dividing the value of the concrete compressive stress by the concrete compressive strain at the corresponding loading stage.

PROCEDURES FOR ESTIMATION OF ULTIMATE DEFORMATION

The value of d_f affects the magnitude of the lateral load. In the case of columns with dominant flexural response, due to the effect of support confinement, a plastic hinge will form a small distance away from the support. This will result in increasing the overall lateral load capacity of the column. This resulted in up to approximately a 20% lateral load reduction for flexure column specimens studied in this paper. Therefore, the authors believe that this adjustment needs to be employed in the analysis.

NUMERICAL EXAMPLES

The analytical results in Fig. 11 are the ultimate points of deformations and loads for the column specimens. As mentioned previously, the ultimate deformation capacity approach presented in this paper can be implemented only for evaluation of the load and deformation of the columns at the ultimate stage. Although one may try to estimate pre- or post-peak response of the column by implementing a small modification in the current method, it has not been verified for full load deformation response analysis. This method is a simplification of the original ASFI method, which is a method capable of doing full load deformation analysis.[3] As mentioned in the paper, for columns with very low shear stress (those are columns with very high shear capacity and very low flexure load), the compression softening factor β is limited to 0.15. This means the method overestimates the ultimate deformation for these columns. Further studies and modifications are needed for the method in this regard.

It is important to note that comprehensive analysis software has been developed at the University of Toronto, based on the MCFT, which is capable of predicting the entire load deformation response, including under cycling loading regimes.[16]

REFERENCES

16. Palermo, D., and Vecchio, F. J., "Compression Field Modeling of Reinforced Concrete Subjected to Reversed Loading: Verification," *ACI Structural Journal*, V. 101, No. 2, Mar.-Apr. 2004, pp. 155-164.

Disc. 106-S23/From the March-April 2009 *ACI Structural Journal*, p. 215

Evaluation of Bundled Bar Lap Splices. Paper by Tarek R. Bashandy

Discussion by Andor Windisch

ACI member, PhD, Karlsfeld, Germany

The author should be complimented for his interesting test series. In explaining the background, however, one important influencing factor in splicing members in flexure was not mentioned: the horizontal splitting of the concrete cover at the end of the spliced reinforcing bar due to the reinforcing bar's bending stiffness. At the very end of a spliced reinforcing bar, the curvature must "jump" from zero to the finite curvature in the member. At the jump, a theoretically infinite transversal force must develop that lets the cover horizontally crack. This crack mobilizes the transverse (confining) reinforcement positioned mainly at the ends of the splice length. The greatest influence of the concrete cover is its resistance in tension. The influence of the side concrete cover and the clear spacing can easily be understood.

It is obvious as well that the flexural rigidity of one 32 mm diameter (No. 10) reinforcing bar is four times higher than that of four 16 mm diameter (No. 5) reinforcing bars. This explains the increasing failure loads with an increasing numbers of bars in the bundle without stirrups.

Comparing Fig. 2 and 4, some doubt may arise concerning the effective bond areas: along the splice, the contact of the bundles substantially reduces the surface embedded in concrete. The efficient perimeter ratios are 1:1.06:1.0:1.25, that is, the three-bar bundle has the same bond area as the single bar. Nevertheless, this deviation can not be realized in the experimental program, as the failures were not bond governed as revealed comparing the average measured steel stresses of the specimens in Groups 1 and 4.

Figure 6(a) reveals that (at least) Beams B7 to B9 were still uncracked in flexure as the failure due to splitting crack (refer to Fig. 5) occurred. The average measured steel stresses at P_{max}, shown in Table 1, are still far away from the yield strength of the reinforcing bars.

The distribution of stresses among bars in the bundle reflects the position of the bars related to the neutral axis only, (refer to Fig. 8(a) and (c)). Certainly, the position of the strain gauges with regard to the flexural axis of the reinforcing bars influences the measured strains.

The authors' test results confirmed the requirement of ACI 318-05 concerning the application of stirrups or ties along the splice length. The author is correct: additional tests with steel yielding are required to confirm the validity of the conclusions of this study. Until then, the bar cutoffs within the bundle should be staggered.

AUTHOR'S CLOSURE

The purpose of the paper was to evaluate the behavior of bundled bar lap splices compared with splices of single bars. The horizontal splitting at the end of the splice described in the discussion occurs in both bundled and single bar splices, but was parallel to the transverse reinforcement (and did not cross it) and therefore did not develop any force in this reinforcement. The horizontal crack at the end of the splice did not affect the splice strength for all types of splices.

There was no correlation between the flexural rigidity of the spliced bars and the splice strength. Although two- and three-bar bundles have lower rigidity compared to single bars, the failure load was generally not higher than equivalent-diameter single-bar bundles. Increasing the number of bars from an equivalent-diameter single bar to two- or three-bar bundle did not increase the failure load. However, four-bar bundles had the lowest rigidity but their failure load was higher than equivalent-diameter single bars. All failures were governed by bond, as indicated by the cracking pattern; sudden failure mode; and examining the specimens after easily removing the concrete cover. It is not possible to draw direct conclusions by directly comparing Groups 1 and 4 because there are variations in two parameters (splice length and concrete cover). The author agrees with the discusser that the variations of effective parameter did not directly affect the failure load. This was presented in the second conclusion.

All specimens were cracked at a relatively low load (20 to 25% of the failure load). This can be concluded by examining the rate of change of bar stresses in Fig. 8, which indicates that flexural cracks occurred at approximately 20 kN (4.5 kips) load. It is not possible to draw conclusions regarding cracking load from Fig. 6 due to the small scale and the relatively low load and deflection at cracking. Figure 5 shows the specimen after failure and removing load; therefore, thin flexural cracks could not be captured in comparison with the wide splitting crack, especially cracks that were not marked.

The distribution of stresses among bars in the bundle had no consistent correlation with the position of the bars related to the neutral axis. For example, in Fig. 8(b), bars placed at the same distance from the neutral axis did not have the same stress. Moreover, the bar closer to the neutral axis had higher stress than one of the bars at a further position from the neutral axis. As presented in this study and the referenced previous study, there were no consistent trends in the distribution of stress within a bundle between bars at the same depth within the section.

Additional tests with steels yielding are required to understand the distribution of stresses among bars in a bundle. However, conclusions regarding bond strength of bundles cannot be drawn from specimens in which steel yields before bond failure. Nevertheless, additional tests with steel stress close to yield are required to confirm the validity of the conclusions of this study.